Photodetachment of H^- in the presence of a low-frequency laser field

S. Bivona, R. Burlon, and C. Leone
Dipartimento di Energetica ed Applicazioni di Fisica, Parco D'Orleans, 90128 Palermo, Italy
(Received 22 July 1991)

The photodetachment of a model one-electron ion simulating H^- in the presence of a low-frequency field is analyzed. Two different geometries are considered in order to get information on the effect of the ponderomotive energy shift Δ on the photodetachment cross section. Our calculations suggest that a correspondence may be established between the ponderomotive shift and the photodetachment cross section, when the ejected electron may exchange only a few low-frequency photons. This is in qualitative agreement with recent experimental observations. When a large number of processes are open in which the detached electron may exchange low-frequency photons with comparable probability, it is impossible to make any connection between ponderomotive threshold shift and photodetachment cross section which, instead, may be described in terms of a field picture.

PACS number(s): 32.80.Rm

I. INTRODUCTION

During the last few years a great deal of experimental and theoretical studies of one-color multiphoton ionization have been performed. The observed photoelectron energy spectra have shown that, when the ionizing radiation intensity is increased, an increase of the minimum number of photons is required in order to strip one electron from the atom [1]. This occurs because the kinetic energy of a free electron in the presence of an electromagnetic field is larger than the average translation energy for the addition of the energy associated with the wiggle motion. Hence, ionization of an atom by an intense radiation field requires the absorption of more energy than the electron's binding energy because, in addition, the quiver energy Δ, which may be considered as the ionization threshold shift, must be supplied. It has been invoked to explain the disappearance of the lowest-energy photoelectron peaks in above-threshold ionization experiments [2]. Generally, such shifts are not observed in those experiments in which use is made of a long-pulse field because the quiver energy is transformed into translation kinetic energy during the time in which the electron leaves the interaction volume. On the other hand, evidence of the shift is clearly given in the experiments with picosecond-long pulses [3].

Recently, the observation of the continuum threshold shift has been attempted by a two-color photodetachment of negative chlorine ions [4,5] by a weak field of variable frequency ω_H in the presence of a strong microwave or infrared field of frequency ω_L and amplitude E_L which provides the threshold shift $\Delta = e^2 E_L^2/(4m\omega_L^2)$. The experimental results may be summarized as follows.

When the ions were photodetached in the presence of the infrared radiation, a sizable detachment rate was measured below the field-free threshold because the negative ions, besides one ultraviolet photon, might simultaneously absorb one or more infrared photons. Above the field-free threshold, a photodetachment rate less than the field-free one was measured, which, however, increased with the ultraviolet frequency ω_H. The slope of the curve showing the photodetachment rate as a function of ω_H changes very suddenly when the difference between the energy of the ultraviolet photon and the field-free threshold amounted to about one-third of the expected shift due to the ponderomotive effect. So, while the change in the slope may be attributed to the opening of the photodetachment with no exchange of infrared photons, its occurrence at values of ω_H lower than the expected ones was related to the spatial inhomogeneity of the infrared illumination. In fact, those negative ions far from the central region of focalization of the infrared radiation which experienced a weaker radiation field and, hence, a smaller ponderomotive shift were detached, giving a contribution to the photodetachment signal after absorbing a single ultraviolet photon whose frequency was closer to the field-free frequency threshold.

When the chlorine ions were detached in the presence of a microwave field, a threshold shift was reached of about 15 eV. Again, the detachment signal was observed at values of the ultraviolet-photon energy lower than the field-free energy threshold, and well above the field-free threshold, photodetachment rates were measured and their values were found to fluctuate about the zero-field ones. Hence, no relationship between the threshold shift and the observed photodetachment cross sections could be established.

In order to explain these experimental results, calculations have been performed by using one-dimensional model ions [6,7]. The calculated two-color photodetachment probabilities plotted as a function of ω_H do not show a sharp threshold, though this function changes very suddenly in slope when $\hbar\omega_H$ is roughly equal to the field-free detachment energy plus the ponderomotive energy shift (however, the change in the slope tends to soften when the low-frequency field intensity increases).

Recently, calculations of two-color photodetachment probabilities have been performed by considering the negative ion of hydrogen [8], for which accurate representation of both the ground state and continuum states

exists. The reported results suggesting the evolution of the photodetachment probability cannot be described in terms of an energy-threshold shift and, consequently, appear to be in contrast to the conclusion of Ref. [6].

Therefore, the understanding of the evolution of the photodetachment probability of negative ions near the threshold may be considered a problem still open. The aim of the present paper is to accomplish this task.

As suggested by the analysis of the experimental results of Ref. [4], it is more convenient to study the problem under two different regimes characterized by the ratio $\Delta/\hbar\omega_L$ which, for ω_H near the field-free threshold, corresponds to the minimum number of low-frequency photons the ions must absorb to be detached. Below, it will be shown that, when $\Delta\hbar\omega_L \ll 1$, the ejected electron may exchange only few low-frequency photons, while in the opposite case, when $\Delta\hbar\omega_L \gg 1$, a large number of channels is open in which the detached electrons may exchange low-frequency photons with, roughly, an equal probability. In these two quite distinct regions, the behavior of the cross sections versus ω_H is expected to be very different.

For simplicity, we assume a single-electron model ion defined by a three-dimensional δ-function potential which, as is well known, supports only one bound state whose energy, in our model, has been chosen to be $I_0=-0.75$ eV, equal to the binding energy of H^-. Further, we use the Keldish approximation [9] in the $\mathbf{E}\cdot\mathbf{r}$ gauge, which has been found to give accurate results in this kind of problem [10] and is based on the following physical picture: the bound electron, after absorbing simultaneously one photon of high frequency and exchanging n photons of low frequency, decays into the continuum through a single-step process.

II. THEORY

In this section we derive the photodetachment cross sections by a weak field of frequency ω_H in the presence of strong radiation laser field of low frequency ω_L.

In the E gauge, the Schrödinger equation for one electron in the presence of a static potential $V(r)$ and two coherent radiation fields, taken in dipole approximation, is written as

$$\left[\frac{i\hbar\delta}{\delta t}-H_0-W_L(r,t)-W_H(r,t)\right]\Psi(r,t)=0 \tag{1}$$

with

$$H_0=p^2/2m+V(r) \tag{2}$$

the unperturbed Hamiltonian and

$$W_H(r,t)=e\mathbf{r}\cdot\mathbf{E}_H\exp(-i\omega_H t) \tag{3}$$

and

$$W_L(r,t)=e\mathbf{E}_L\cdot[\hat{\xi}_\alpha\sin\omega_L t\cos(\zeta/2) -\hat{\xi}_\beta\cos\omega_L t\sin(\zeta/2)] \tag{4}$$

the interactions of the ion with the two fields. E_j $(j=H,L)$ are the electric amplitudes, ζ the polarization parameters, $\hat{\xi}_\alpha$ and $\hat{\xi}_\beta$ two unit vectors along two perpendicular directions. In the following, the high-frequency field will be taken to be linearly polarized along the z axis.

Though Eq. (1) does not exhibit any periodicity, solutions may be obtained which are analogous to the quasienergy states, by considering the following eigenvalue problem:

$$\left[\frac{i\hbar\delta}{\delta t_1}+\frac{i\hbar\delta}{\delta t_2}-H_0-W_L(r,t)-W_H(r,t)\right]\Phi_E(r,t_1,t_2) =E\Phi_E(r,t_1,t_2)\ . \tag{5}$$

The wave function $\Phi_E(r,t_1,t_2)$ is periodic with respect to the variables t_1 and t_2, and the wave function

$$\Psi_E(r,t)=\lim_{\substack{t_1\to t\\ t_2\to t}}\exp(-iEt/\hbar)\Phi_E(r,t_1,t_2) \tag{6}$$

may be shown to be a solution of the Schrödinger equation (1) [11]. Though $\Psi_E(r,t)$ is not periodic, it may be considered as some stationary state of the model ion in the presence of two radiation fields.

For low intensity of the high-frequency radiation, the interaction $W_H(r,t)$ may be treated perturbatively and its action is responsible for the electron transitions between quasienergy states. At the first order of the perturbation theory in $W_H(r,t)$, the amplitude of photodetachment probability from the bound state with absorption of one photon ω_H and exchange of n photon ω_L is given by

$$A_{qi}(n)=\langle\langle\,\phi_q(r,t)\exp(-in\omega_L t)|e\mathbf{E}_H\cdot\mathbf{r}|\phi_0(r,t)\,\rangle\rangle\ , \tag{7}$$

where

$$\langle\langle\ \cdots\ \rangle\rangle=(2i/\omega_L)\int_0^{2\pi}dt\langle\ \cdots\ \rangle \tag{8}$$

and $\langle\ \cdots\ \rangle$ indicates space integration only; $\phi_0(r,t)$ and $\phi_q(r,t)$ are the periodical part of the quasienergy states, which tend, respectively, to the field-free ionic ground state $u_0(r,t)$ and to the state $u_q(r,t)$ with kinetic energy

$$\hbar^2q^2/2m=\hbar\omega_H+n\hbar\omega_L+I_0-\Delta+\delta I_0 \tag{9}$$

when the low-frequency electric field is switched off; δI_0 is the dynamic Stark shift of the bound state.

For the attractive three-dimensional δ-function potential, the spatial part of the wave function of the field-free bound state is taken as [12]

$$u_0(r)=B\left[\frac{b}{2\pi}\right]^{1/2}\frac{\exp(-br)}{r}\ , \tag{10}$$

where

$$b=(2mI_0)^{1/2} \tag{11}$$

and B is an empirical constant with the value [12]

$$B^2=2.65\ . \tag{12}$$

As this bound state is single and well separated from the continuum, the dressed bound quasienergy state in the presence of a low-frequency radiation field may be constructed by the method of Ref. [13]:

$$\Psi_0(r,t)=\exp[i/\hbar(I_0+\delta I_0)t]\phi_0(r,t)\ . \tag{13}$$

The Stark shift of the bound state δI_0 may be approximated at the second order of perturbation as [13]

$$\delta I_0=\alpha_s E_0^2/4 \tag{14}$$

with α_s the static-dipole polarizability and

$$\phi_0(r)=u_0(r)\exp[-(\delta I_0/2\omega_L)\cos\zeta\sin2\omega_L t]\ . \tag{15}$$

The continuum quasienergy states in the presence of a static δ potential and a low-frequency radiation field may be well approximated by the Volkov solution

$$\Psi_q(r,t)=\exp[-i/\hbar(\hbar^2q^2/2m+\Delta)t]\phi_q(r,t) \tag{16}$$

with

$$\phi_q(r,t)=(2\pi)^{-3/2}\exp\{i[\mathbf{q}-\mathbf{K}_L(\omega_L t)]\cdot\mathbf{r}\} \times\exp\{i[\lambda_q(\omega_L t)+\rho(\omega_L t)\cos\zeta]\}\ , \tag{17}$$

$$\mathbf{K}_L(\omega_L t)=[eE_L/\hbar\omega_L)][\hat{\xi}_\alpha\cos(\omega_L t)\cos(\zeta/2) +\hat{\xi}_\beta\sin(\omega_L t)\sin(\zeta/2)]\ , \tag{18}$$

$$\lambda_q(\omega_L t)=[eE_L/(m\omega_L^2)][\hat{\xi}_\alpha\sin(\omega_L t)\cos(\zeta/2) -\hat{\xi}_\beta\cos(\omega_L t)\sin(\zeta/2)]\cdot\mathbf{q}\ , \tag{19}$$

$$\rho(\omega_L t)=[e^2E_L^2/(8m\omega_L^2)]\sin2\omega_L t=\rho\sin2\omega_L t\ . \tag{20}$$

Proceeding in the usual way, the differential and total photodetachment cross sections with absorption of one photon of frequency ω_H and exchange of n photons ω_L are, respectively, obtained as

$$\frac{d\sigma(n)}{d\Omega}=(m\omega_H e^2 q_n/\hbar^2 c)|T_n(\mathbf{q}_n,\mathbf{K}_L)|^2\ , \tag{21}$$

$$\sigma(n)=\int\frac{d\sigma(n)}{d\Omega}d\Omega\ , \tag{22}$$

where

$$T_n(\mathbf{q}_n,\mathbf{K}_L)=\int_{-\pi}^{+\pi}d\alpha\, f_n(\alpha)M(\mathbf{q}_n,\mathbf{K}_L(\alpha))\ , \tag{23}$$

$$f_n(\alpha)=\exp[in\alpha+i\lambda_q(\alpha)-i\rho\sin(2\alpha)\cos\zeta]\ , \tag{24}$$

$$\bar{\rho}=\rho-\alpha_s E_0^2/(8\omega_L)\ , \tag{25}$$

$$M(\mathbf{q}_n,\mathbf{K}_L(\alpha)) =-iB(b/\pi^2)^{1/2}[\mathbf{q}-\mathbf{K}_L(\alpha)]\cdot\hat{\mathbf{z}}/[b^2+|\mathbf{q}-\mathbf{K}_L(\alpha)|^2]^2\ , \tag{26}$$

$$h^2q_n/2m=n\hbar\omega_L+\hbar\omega_H+I_0-\bar{\Delta}\ , \tag{27}$$

and

$$\bar{\Delta}=\Delta-\delta I_0\ . \tag{28}$$

Equation (27) shows that the photodetachment channel, in which a given number of low-frequency photons are exchanged, opens at a threshold energy given by

$$\hbar\omega_{\text{th}}(n)=-n\hbar\omega_L-I_0-\delta I_0+\Delta\ . \tag{29}$$

Summing over all the channels, the photodetachment cross section is obtained as

$$\sigma=\sum_n\sigma(n)\ . \tag{30}$$

In the following calculations, for the choice of laser parameters, the dynamic Stark shift is found to be much less than the ponderomotive potential and, then, will be disregarded.

III. RESULTS AND COMMENTS

The treatment developed in the previous section is now applied to study the behavior of the total cross section of photodetachment into a given channel as a function of the radiation frequencies and of the intensity of the low-frequency radiation. Further, it gives the possibility to get information about the way in which each channel contributes to the photodetachment process.

As already mentioned in the Introduction, the experimental results of Ref. [4] have singled out two different situations which, ultimately, differ strongly in the number of channels which contribute to the ejection of the electron (a couple of channels in the case of irradiation by 1.17-eV energy photons against millions of channels participating to the photodetachment in the presence of a microwave field).

Therefore, we choose to carry out calculations in two different regimes characterized by a proper combination of the frequency and intensity of the low-frequency laser field. They may be defined by the ratio $\Delta/\hbar\omega_L$, which, for $h\omega_H$ near the field-free threshold, gives the minimum number of photons that the electron must absorb to be ejected. When $\Delta/\hbar\omega_L\ll1$, the ejected electrons may exchange only few low-frequency photons, while in the opposite case when $\Delta/\hbar\omega_L\gg1$, a large number of channels is open in which the detached electrons may exchange low-frequency photons with comparable probability.

For all the cases considered below, the weak high-frequency field is taken to be linearly polarized along $\hat{\mathbf{z}}$, while the following polarizations and geometries will be considered for the low-frequency field: (a) the low-frequency field is linearly polarized (the polarization parameter $\zeta=0$), and the two fields are parallel $(L,\|)$; (b) the low-frequency is circularly polarized (the polarization parameter $\zeta=\pi/2$) with the polarization plane coinciding with the plane (x,y). Accordingly, it is perpendicular to the high-frequency electric-field polarization direction $(C_{xy},\perp)$.

A. Regime $\Delta/\hbar\omega_L\ll1$

In Figs. 1(a) and 2(a), we show photodetachment cross sections and total cross sections of photodetachment into channels with $|n|=0$, 1, 2 as a function of ω_H. We limit our consideration to these channels as, for the laser parameters we have chosen, processes involving a larger number of low-frequency photons can be neglected. Accordingly, this may be considered a perturbative regime.

For both the geometries described above, the curves relative to the photodetachment cross sections show a

rather abrupt change in the slope at the value of the high-frequency energy $\hbar\omega_H=\Delta-\delta I_0+I_0$ corresponding to the energy of the field-free threshold shifted by the ponderomotive potential Δ and the dynamic Stark shift of the bound state δI_0. Of course, the sudden change of the cross section is due to the opening of the photodetachment channel with $n=0$ whose cross section near the threshold rises as $(\omega_H-\omega_{\rm th})^{3/2}$, according to the Wigner threshold law. As far as the channels with $|n|=1$ are concerned, we note that the corresponding cross sections display a behavior which depends on the geometrical arrangements of the em fields. In fact, when, in addition to the high-frequency photon, one circularly polarized photon is absorbed, the electron is ejected in a state with orbital quantum number $l=2$ and the cross section exhibits a $(\omega_H-\omega_{\rm th})^{l+1/2}$ dependence, whereas in the case of parallel geometry the dominant contribution to the cross section coming from the partial s wave gives rise to a $(\omega_H-\omega_{\rm th})^{1/2}$ dependence. This is displayed in Figs. 1(b) and 2(b) where it is also shown that, beyond the threshold, but not too far from it, for the geometry $(L,\|)$ the cross section involving the emission of one low-frequency photon has a different behavior from the one involving the absorption on one low-frequency photon. In particular, the cross section of this last process, after increasing, reaches a plateau and then starts increasing again with ω_H, while the curve relative to the other process increases monotonically with ω_H. Instead, for the geometry $(C_{xy},\perp)$ the cross sections with absorption and emission of the same number of low-frequency photons behave quite similarly. All these features can be explained as follows. As $\Delta/\hbar\omega_L\ll 1$, for the $(L,\|)$ geometry, we may neglect ρ in Eq. (24). Further, by approximating Eq. (26) as

$$M(\mathbf{q}_n,\mathbf{K}_L(\alpha))=B(b/\pi^2)^{1/2}[\mathbf{q}-\mathbf{K}_L(\alpha)]\cdot\hat{\mathbf{z}}/b^4 \tag{31}$$

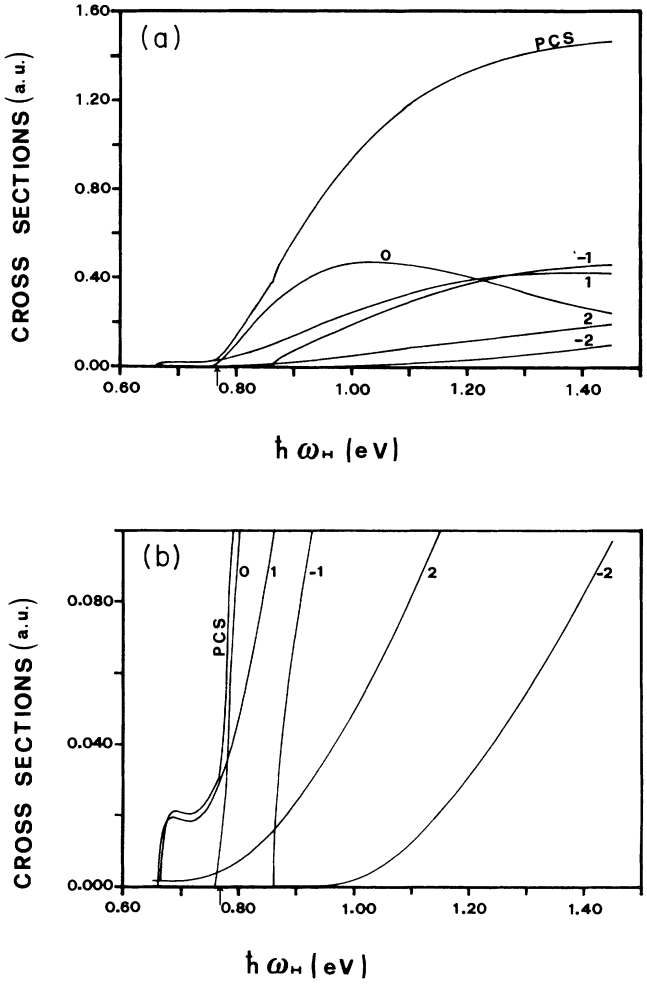

FIG. 1. (a) Photodetachment cross section (PCS) and total cross sections of photodetachment with exchange of low-frequency laser-field photons as a function of ω_H for the $(L,\|)$ geometry (regime $\Delta/\hbar\omega\ll 1$). The numbers on the curves denote the number of exchanged low-frequency photons. The parameters of the low-frequency laser field are $I_L=7\times10^8$ W/cm^2, $\hbar\omega_L=0.1$ eV. (b) The same as (a).

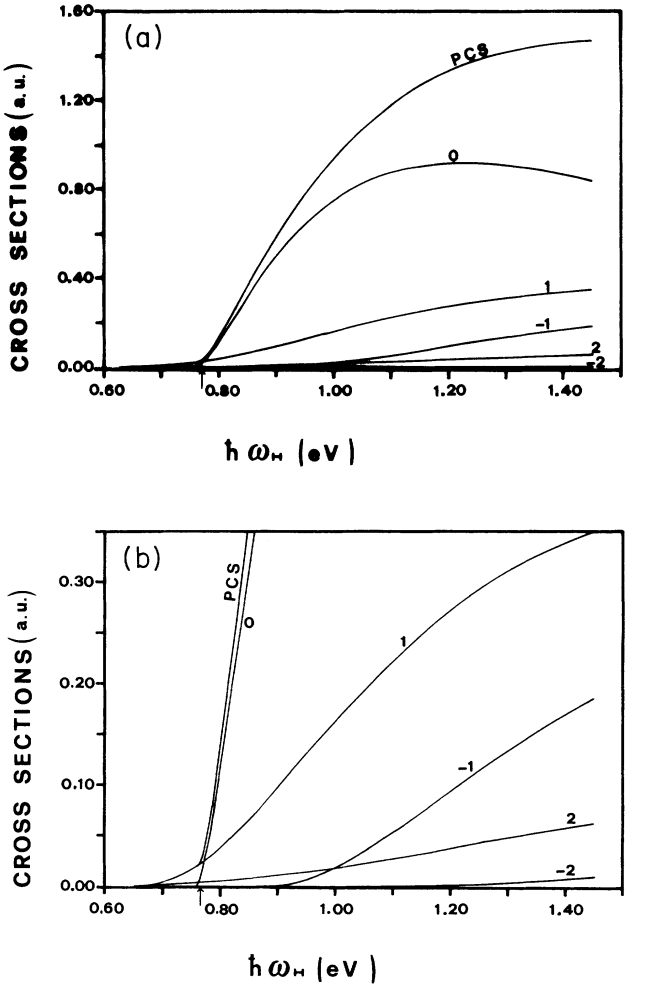

FIG. 2. (a) Photodetachment cross section and total cross sections of photodetachment with exchange of low-frequency laser-field photons as a function of ω_H for the $(C_{xy},\perp)$ geometry (regime $\Delta/\hbar\omega\ll 1$). The numbers on the curves denote the number of exchanged low-frequency photons. The parameters of the low-frequency laser field are the same as in Fig. 1(a). (b) The same as (a).

and integrating Eq. (23), the differential cross section Eq. (21) is obtained as

$$d\sigma(n)/d\Omega=(4B^2b^{-7}m\omega_H e^2q_n/h^2c)\times J_n^2(\lambda_q)(q\cos\theta-nm\omega_L/\hbar q\cos\theta)^2 , \quad (32)$$

where

$$\lambda_q=(e/m\omega_L^2)\mathbf{E}_L\cdot\mathbf{q} . \quad (33)$$

θ is the angle between q and z, and $J_n(\lambda_q)$ the Bessel function of integer order. The second term in the last parenthesis results from integrating the term $\mathbf{K}_L(\alpha)$ entering Eqs. (23) and (26) which gives rise to constructive interference when $n<0$, and to a destructive interference when $n>0$. For the geometry $(C_{xy},\perp)$ $\mathbf{K}_L(\alpha)\cdot\hat{\mathbf{z}}$ and ρ entering, respectively, Eqs. (26) and (24), are both zero, and Eq. (21) becomes

$$d\sigma(n)/d\Omega=(4B^2b^{-7}m\omega_H e^2q_n/\hbar^2c)J_n^2(\lambda_{q_\perp})(q\cos\theta)^2 \quad (34)$$

with

$$\lambda_{q_\perp}=eE_Lq\sin(\theta)/(m\omega_L^2) . \quad (35)$$

From Eq. (34), total cross sections are obtained for photodetachment involving the same number of absorbed or emitted photons which exhibit the same behavior when the corresponding channels open. Moreover, we note that, in this geometry, the coupling strength between the em field and the ejected electron is weaker than in the $(L,\|)$ geometry. As a consequence, the influence of the intense laser field on the photodetachment cross section is more effective in the parallel geometry.

In Fig. 3, photodetachment cross sections are reported for different values of the ponderomotive shift of the threshold Δ and different values of ω_L, but all chosen in such a way that the ratio $\Delta/\hbar\omega_L=0.1$ is kept fixed. The main result found in this regime is that all the curves change suddenly in slope when $\hbar\omega_H=\Delta+I_0$, showing that a tight connection between the photodetachment cross sections and the ponderomotive shift may be established. In this sense, our calculations show that, at least in the regime $\Delta/\hbar\omega_L\ll1$, theory and experimental results can be considered in good qualitative agreement.

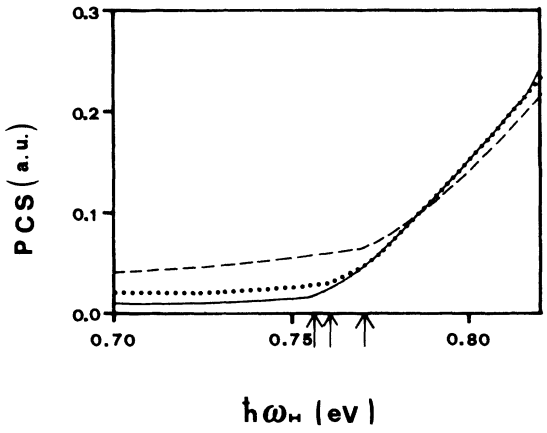

FIG. 3. Photodetachment cross sections for the geometry $(L,\|)$ as a function of ω_H for different ω_L. The ratio $\Delta/\hbar\omega_L=0.1$ is kept fixed. The positions marked by the arrows correspond to the values of the ionization energy shifted by Δ. Solid curve, $\hbar\omega_L=0.06$ eV; dotted curve $\hbar\omega_L=0.1$ eV; dashed curve, $\hbar\omega_L=0.2$ eV.

B. Regime $\Delta/\hbar\omega_L\gg1$

This is a highly nonlinear regime. Hence, a considerable number of low-frequency photons may be absorbed during the photodetachment event. This circumstance marks the differences from the previous examinated case. In fact, when $\Delta/\hbar\omega_L\gg1$, the photoelectron signal may be sizable well before ω_H reaches the field-free threshold, as the ponderomotive energy shift may be overcome by the absorption of numerous low-frequency photons. Consequently, the ponderomotive energy shift is expected to no longer be a useful parameter for describing the behavior of the photodetachment cross section. This is illustrated in Figs. 4 and 5. In Fig. 4, the photodetachment cross sections are shown for the $(L,\|)$ geometry as a function of ω_H for a fixed intensity and several frequencies of low-frequency laser, while in Fig. 5 the same quantity is shown for different intensities at the same ω_L. We remark that (see Fig. 4), by varying ω_L over a wide range of values, the cross sections do not change appreciably, while considerable modifications appear when the low-frequency laser intensity is varied at a fixed value of ω_L. A quite similar result is obtained in the perpendicular $(C_{xy},\perp)$ geometry (see Fig. 6), though the low-frequency laser field has a reduced effect on the photodetachment

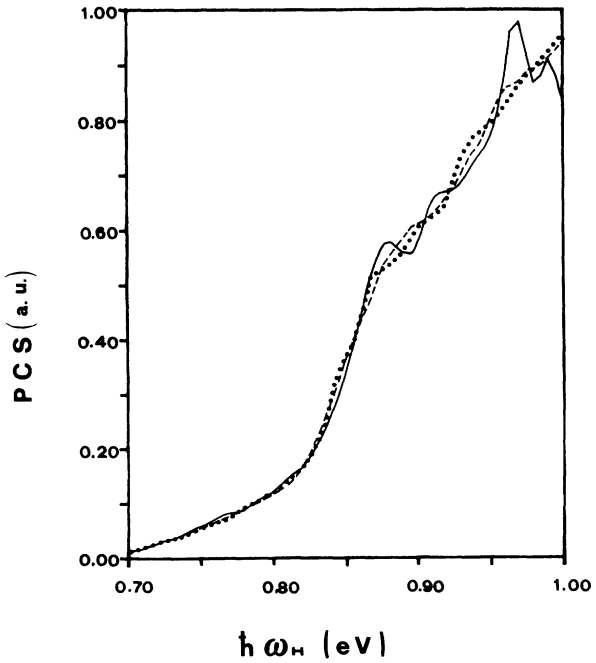

FIG. 4. Photodetachment cross sections for the geometry $(L,\|)$ as a function of ω_H for different frequencies ω_L at a fixed value of the low-frequency field intensity $I_L=5\times10^8$ W/cm^2 (regime $\Delta/\hbar\omega_L\gg1$). Solid curve, $\hbar\omega_L=0.01$ eV; dotted curve, $\hbar\omega_L=0.02$ eV; dashed curve, $\hbar\omega_L=0.03$ eV.

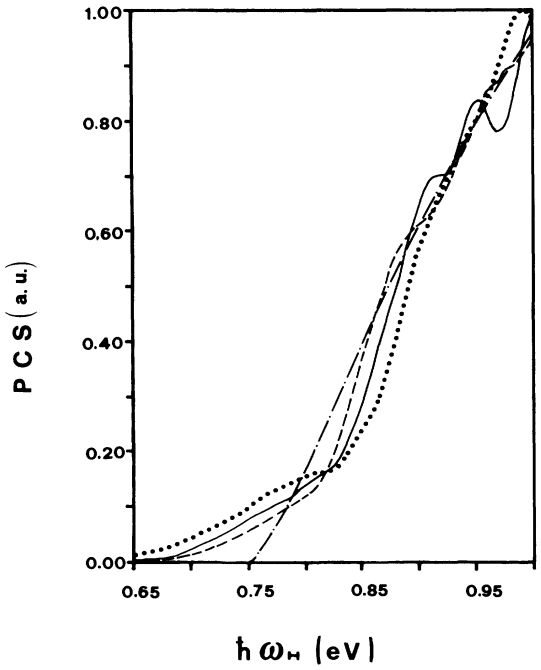

FIG. 5. The same as Fig. 4 for different values of the low-frequency field intensity at a fixed value of ω_L ($\hbar\omega_L = 0.02$ eV). Solid curve $I_L = 10^9$ W/cm^2; dotted curve, $I_L = 2\times 10^9$ W/cm^2; dashed curve, $I_L = 5\times 10^8$ W/cm^2; dot-dashed curve, field-free photodetachment.

event as compared to the case in which the high- and low-frequency fields oscillate along the same direction. The curves shown in Figs. 5 and 6 are slowly increasing functions of ω_H within a range of values which includes the field-free threshold frequency and which becomes wider as the low-frequency intensity increases. Well

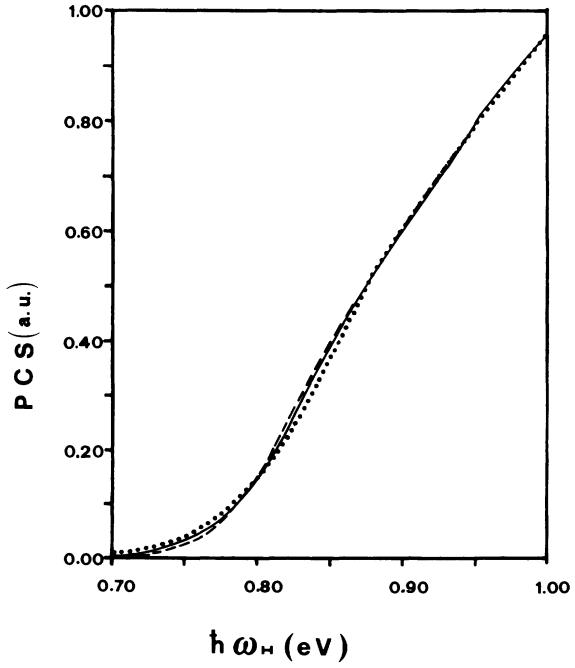

FIG. 6. The same as Fig. 5 for the (C_{xy},$\perp$) geometry.

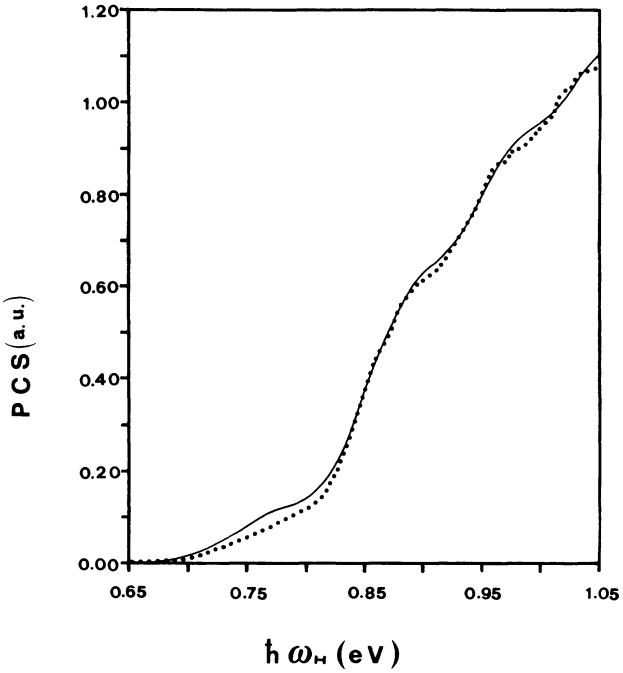

FIG. 7. Comparison between photodetachment cross section obtained by Eq. (30) (regime $\Delta/\hbar\omega_L \gg 1$) and numerical averages of the photodetachment cross section in a static electric field. The low-frequency field intensity is $I_L = 5\times 10^8$ W/cm^2. Solid curve, photodetachment in the presence of a static field; dotted curve, photodetachment cross section in the presence of the laser field.

above the field-free threshold, the photodetachment signal is depressed as compared to the field-free one. By ulteriorly increasing ω_H, a region is reached in which the cross sections rise very suddenly and eventually oscillate about the field-free results. This behavior is reminiscent of the photodetachment in the presence of a static electric field. On the other hand, the above remarked poor sensitivity of the photodetachment cross section to the variation of the low frequencies can be considered a manifestation of the quasistaticity of the process whose cross section should be roughly the same as the one obtained by averaging, over a period of the low-frequency field, the cross section for a static field.

The consistency of this assumption was experimentally verified by the authors of Ref. [4], and the results presented below may be considered as a corroboration. In Figs. 7 and 8, a comparison is shown between the cross section obtained by Eq. (30) in the (L,$\|$) geometry and numerical averages σ_A of the photodetachment cross section in a static electric field given by

$$\sigma_A = \frac{2}{\pi}\int_0^{\pi/2} \sigma_{ff}(E_L \sin\alpha)\, d\alpha \ , \tag{36}$$

where σ_{ff} is the photodetachment cross section in a static electric field whose intensity is E [14,15],

$$\sigma_{ff}(E) = 0.3604 \frac{E}{\omega_H^3} D[2^{1/3}(\omega_H - I_0)/E^{2/3}] \ . \tag{37}$$

In Eq. (37), atomic units have been used,

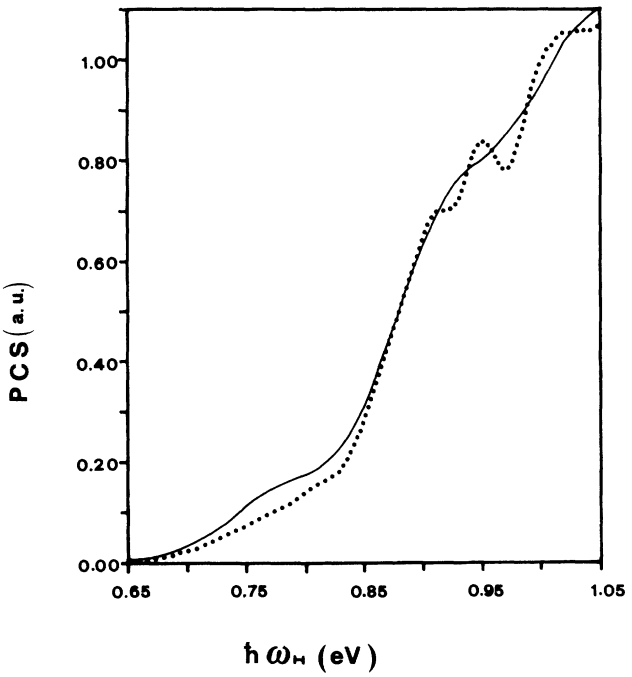

FIG. 8. The same as Fig. 7 for $I_L = 10^9$ W/cm^2.

$$D(x) = \int_{-\infty}^{x} \left[\frac{d}{dz} A_i(-z) \right]^2 dz \tag{38}$$

and $A_i(t)$ is the Airy function.

The curves are quite similar and their differences are expected to become less and less when ω_L decreases. Finally, this last result may be considered to be the analog of the above-threshold-multiphoton ionization in the high-intense filed regime, when the electron ejection may be described in terms of tunnel effect or, accordingly, the field picture rather than the photon picture may be used.

IV. CONCLUDING REMARKS

We have analyzed the multiphoton detachment of a model one-electron ion simulating H^- by two em fields, arranged in two different geometries in order to get information on the effect of the ponderomotive energy shift Δ on the photodetachment cross section. Our results suggest that, in the perturbative regime, when $\Delta/\hbar\omega_L \ll 1$, a correspondence may be established between the ponderomotive shift and the photodetachment cross section.

Recent experimental observations have shown that a qualitative agreement exists between the expected threshold and the experimental results. When in the highly nonlinear region ($\Delta/\hbar\omega_L \gg 1$) where many processes with a large number of photons participate in the photodetachment event, it is impossible to make any connection between ponderomotive threshold shift and photodetachment cross section which, instead, may be described in terms of field picture.

ACKNOWLEDGMENTS

The authors express their thanks to the University of Palermo Computational Center for the computer time generously provided to them. This work was supported in part by the Italian Ministry of Education, The National Group of Structure of Matter and the Sicilian Regional Committee for Nuclear and Structure of Matter Researches.

[1] P. Agostini, F. Fabre, G. Mainfray, G. Petite, and N. K. Rahman, Phys. Rev. Lett. **42**, 1127 (1979); P. Kruit, J. Kimman, H. G. Muller, and M. J. van der Wiell, Phys. Rev. A **28**, 248 (1983); T. J. McIlrath, P. H. Bucksbaum, R. R. Freeman, and M. Bashkanski, *ibid.* **35**, 4611 (1987), and references therein; T. F. Gallegher, Phys. Rev. Lett. **61**, 2304 (1988); P. B. Corkun, N. H. Burnett, and F. Brunel, *ibid.* **62**, 1259 (1989).

[2] A number of articles are collected in the feature on multielectron excitation in atoms, J. Opt. Soc. B **4**, 705 (1987).

[3] R. R. Freeman, P. H. Bucksbaum, H. Milchberg, S. Darack, D. Schumacher, and M. E. Gesuic, Phys. Rev. Lett. **59**, 1092 (1987).

[4] D. J. Larson, P. S. Armostrong, M. C. Baruch, T. F. Gallagher, and T. Olson, *Proceedings of the International Conference on the Physics of Electronic and Atomic Collisions,* New York (North-Holland, Amsterdam, 1989), p. 513.

[5] R. Trainham, G. D. Fetcher, N. B. Mansour, and D. J. Larson, Phys. Rev. Lett. **59**, 2291 (1987); M. C. Baruch, T. F. Gallagher, and D. J. Larson, Bull. Am. Phys. Soc. **34**, 1398 (1989).

[6] M. Dorr and R. Shakeshaft, Phys. Rev. A **40**, 459 (1989).

[7] L. A. Bloomfield, J. Opt. Soc. Am. B **7**, 472 (1990).

[8] M. Crance, J. Phys. B **23**, L667 (1990).

[9] L. V. Keldish, Zh. Eksp. Teor. Fiz. **48**, 874 (1965) [Sov. Phys. JETP **21**, 1307 (1965)].

[10] W. Becker, J. K. McIver, and M. Coufer, Phys. Rev. A **40**, 6904 (1989); M. Dorr, R. Potvliege, and R. Shakeshaft, Bull. Am. Phys. **35**, 1183 (1990); W. Becker, Li-E. Li, and J. K. McIver, J. Phys. B **23**, L753 (1990).

[11] N. Manakov V. Ovsiannikov, and L. Ropoport, Phys. Rep. **141**, 430 (1986).

[12] B. H. Armstrong, Phys. Rev. **131**, 1132 (1963); H. R. Reiss, Phys. Rev. A **22**, 1786 (1980).

[13] M. H. Mittleman, Phys. Rev. A **40**, 463 (1989).

[14] M. L. Du and J. B. Delos, Phys. Rev. A **38**, 5609 (1988).

[15] A. R. P. Rau and Him-Yiu Wong, Phys. Rev. A **37**, 632 (1988).